PCCP

PAPER

View Article Online
View Journal | View Issue

Cite this: *Phys. Chem. Chem. Phys.*, 2015, **17**, 4231

A long-term oxidation barrier for copper nanowires: graphene says yes

Liangjing Shi,† Ranran Wang,† Haitao Zhai, Yangqiao Liu,* Lian Gao and Jing Sun*

Received 9th November 2014,
Accepted 23rd December 2014

DOI: 10.1039/c4cp05187d

www.rsc.org/pccp

Copper nanowires (Cu NWs) hold great promise for the fabrication of low-cost transparent electrodes. However, the instability of Cu NWs has limited their application into commercial devices. Herein, CVD-grown graphene is transferred onto Cu NW films and the stability of the hybrid films over long time scale under different conditions is investigated systematically. The results reveal that the graphene–Cu NW films can maintain their efficacy ($R/R_0 < 2$) after 180 days of exposure in an ambient atmosphere. Furthermore, a two-step oxidation kinetic mechanism of Cu NWs can be proposed by using Raman and X-Ray photoelectron spectroscopy. The protecting mechanism of graphene on Cu NW films is disclosed to preventing the oxygen species permeation, decelerating the oxidation from Cu to Cu_2O and hindering the oxidation of Cu_2O to CuO. These results are of referring significance to make metal nanowire based transparent electrodes with both high optical-electrical performance and excellent stability.

1. Introduction

Nowadays transparent electrodes with current drive have been widely used in electronics such as displays, solar cells, touch screens, and LEDs (light-emitting devices). Doped-metal oxide such as tin-doped indium oxide (ITO) is the most commonly used material for transparent conductive electrode (TCE). Recently, there has been a quest of new materials to replace ITO because of the rising cost and its brittleness, which limit its usage in flexible electronic devices.[1] Towards this objective, various alternative materials such as conductive polymers,[2] metal mesh-structures,[3,4] carbon nano-tubes,[5–7] graphene,[8–10] and metal nano-wires[5,11–15] have been studied by different groups. Among these alternatives, metal nanowires have been demonstrated a promising material for transparent electrodes, considering their low cost and high optical-conductive performance which is comparable to or even better than ITO.[14,16–18] Besides, their mesh-like geometries present outstanding mechanical robustness when bent (up to a strain of ~1%)[14,19] or stretched (over a strain of ~50%).[15,20] Among the metal nanowires, silver nanowires are the most intensively researched. Conductive ink and films based on silver nanowires have been commercialized. Flexible electronic devices such as touch screen and OLEDs with high performance have also been constructed based on silver nanowire electrodes.[21] Recently, copper appears as an interesting alternative since it is almost as conductive as silver, however much more abundant and less expensive than silver. Based on these facts, there has been growing interest in the development of copper nanostructures, especially copper nanowires (Cu NWs). The copper nanowires formed networks by wet solution processes, which can facilitate low-cost, high-speed fabrication of transparent electrodes. However, several disadvantages of the copper nanowire films, such as poor adhesion to substrates, typically high junction resistance, high contact resistance between the network (because of the non-contacted, open space in the network) and especially material instability in a severe environment, have limited their applications into commercial devices.[14,19,22] One strategy to overcome the disadvantages of metal nanowire films involves the addition of components like metal nanoparticles, thin metal films, oxide nanostructures, or conductive polymers.[19,23–25]

Graphene owns extremely high electron mobility, but low optical absorption throughout the visible range, which make it a valuable material in electronic area.[26–29] Moreover, graphene was found to be oxygen prohibitive, and several studies have been published to demonstrate the passivation properties of graphene on protecting metals including Cu, Fe, and Ni from oxidation.[30] Nevertheless, some recent studies discovered that graphene was a corrosion protector only for short time, while it promoted long-term oxidation of copper foils at room temperature, since it facilitated the electron transport during the oxidation process.[31,32] As to Cu NWs, they have a rougher surface morphology; also they are more active and easier to be oxidized due to their small diameters. Second, the electron transporting path in the Cu NW network is quite different from that in the flat copper foil. Therefore, whether graphene

State Key Laboratory of High Performance Ceramics and Superfine Microstructure, Shanghai Institute of Ceramics, Chinese Academy of Sciences, 1295 Dingxi Road, Shanghai 200050, People's Republic of China. E-mail: yqliu@mail.sic.ac.cn, jingsun@mail.sic.ac.cn

† These authors contributed equally to the work.

can provide specifically effective protection to the Cu NW network still remains unclear and needs to be investigated systematically.

Herein, we transferred CVD-grown graphene onto Cu NW films, and compared their stability with uncoated Cu NW films over long time scale under different conditions systematically. Evolution of the oxidation process for these films was monitored by Raman spectra and X-ray photoelectron spectroscopy. The protecting mechanism of graphene on the underlying Cu NW films was discussed profoundly. These results are of great importance to understanding the oxidation process of Cu NWs and may shed light on searching optimal strategies to fabricate highly stable metal nanowire films.

2. Results and discussion

2.1 Fabrication and characterization of graphene–Cu NW hybrid films

Cu NWs were synthesized with a solvothermal method reported in our previous work[12] and were made into thin films using a vacuum filtration method with glass slides, silicon wafers and PET sheets as optional substrates. Here, single crystalline silicon wafers were chosen as the substrates since no oxygen and carbon existed in the wafers, which will facilitate the elemental analysis of Cu NW networks. Besides, Cu NW networks were also transferred to polyacrylate substrates by an *in situ* polymerization and a transfer method to reduce the surface roughness and improve the contact between Cu NWs and the above graphene layers. Graphene was fabricated by the CVD process under atmospheric pressure. Typically, the obtained graphene consisted of a single or a few carbon atom layers, with the sheet resistance of about 900–1000 Ω sq^{-1}. The graphene covered Cu NW hybrid films were fabricated through a wet process (as illustrated in Scheme 1), among which glycol–DI water aqueous solution was used as the transfer medium. The ratio between glycol and DI water is critical to the fully extending of graphene.

Inset of Fig. 1c shows a piece of graphene covered Cu NW hybrid film on the polyacrylate substrate. No apparent change was observed compared with bare Cu NW film, which proved that the introduction of graphene did not induce an obvious decrease in optical transmittance over the visible range. This was confirmed by optical spectra. As seen from Fig. 1c, the optical

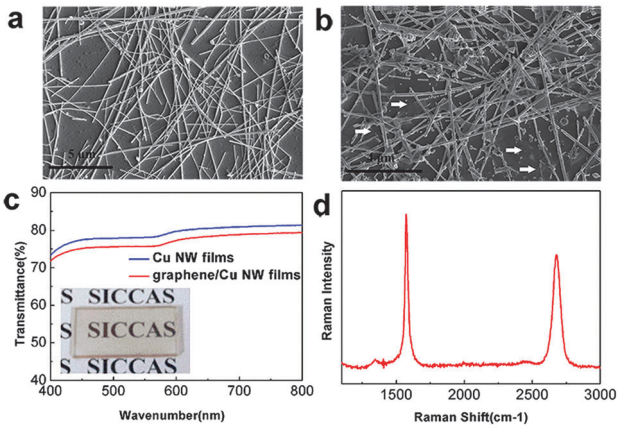

Fig. 1 SEM image of (a) the bare Cu NW films and (b) of the transparent conducting film composed of CVD-grown graphene–Cu NW. (c) Optical transmittance of bare Cu NW films and graphene–Cu NW films on polyacrylate substrates. Inset is the photograph of graphene–Cu NW films on polyacrylate. (d) Typical Raman spectra of graphene on the Cu NW film.

transmittance of the Cu NW film at 550 nm is about 78.1%, and after covering with graphene, the value is about 75.7%. The small decrease of 2.4% indicates that only a single layer of graphene was introduced on the Cu NW film. The Raman spectrum of the graphene–Cu NW film is shown in Fig. 1d. The 2D band (2690 cm^{-1}), the G band (1580 cm^{-1}) and the D band (1350 cm^{-1}) were observed. The intensity ratio of the 2D band to the G band is between 1 and 2, and the intensity of the D band is relatively low, indicating that a single or bi-layer graphene with few defects was introduced. Fig. 1a and b exhibit the SEM images of the Cu NW film before and after covering with graphene. In the bare Cu NW film, long Cu NWs with an average diameter of 80 nm were connected together forming a continuous network, leaving blank spaces between nanowires. After hybrid, the continuous graphene film bestows the whole Cu NW network, filling the blank spaces and bridging unconnected nanowires, as confirmed by the wrinkles in Fig. 1b (marked by white arrows). This would on one hand enhance the conductance of the Cu NW network, since more conducting paths were built. On the other hand, the much larger resistance of the graphene film (about 1000 Ω sq^{-1}) had a deleterious effect on the conductance of the Cu NW network. Taking the two aspects together,

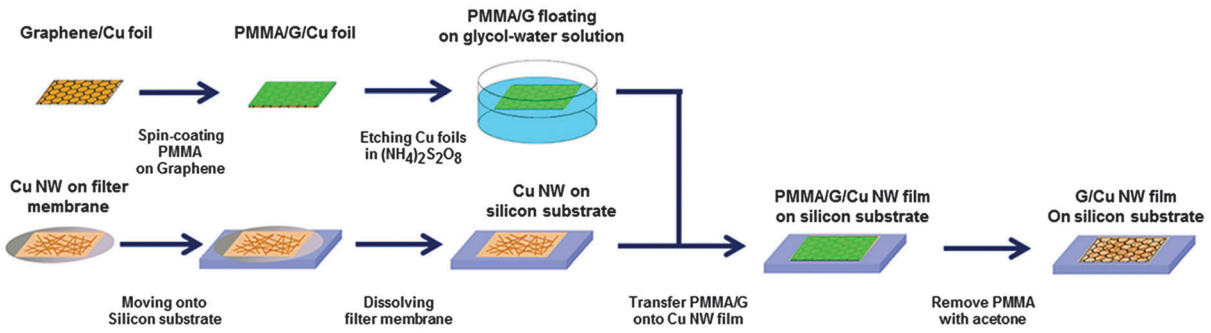

Scheme 1 Preparation of graphene–Cu NW films on silicon substrates.

the sheet resistance of the Cu NW film increased a little after covering with graphene, typically from 11 Ω sq^{-1} to 14 Ω sq^{-1}.

2.2 Oxidation resistance performance

In order to evaluate their oxidation resistance performance, Cu films with and without graphene coverage were stored in an ambient atmosphere and their sheet resistances were measured successively for 6 months. Generally, the ratio of sheet resistance to initial sheet resistance (R/R_0) was used as a test standard. According to previous reports, when R/R_0 becomes larger than 2, the film loses its efficacy as an electrode component. As seen from Fig. 2a, the sheet resistance R of the bare Cu NW film reached the value of $2R_0$ after being kept in air for 8 days due to the oxidation of Cu NWs. That duration reduced to 4 days at elevated temperature (60 °C) owing to the faster oxidation kinetics. In comparison, the graphene covered Cu NW film exhibited much better stability. The ratio of R/R_0 was only 1.27 after being stored in an ambient atmosphere for 45 days, and that ratio was maintained below 2 (1.91) even after 6 months, which testified the long term anti-oxidation effect of graphene. At elevated temperature, the oxidation would be accelerated, even under the protection of graphene. The R/R_0 ratio increased to 1.48 after the film being kept at 60 °C for 35 days, and the hybrid film lost its efficacy (R/R_0 = 14) after 6 months. The stability of the Cu NW film on polyacrylate substrates was found to be better than that on silicon substrates, and the R/R_0 ratio was maintained below 2 for 14 days at room temperature (25 °C). This is attributed to the partly-embedding of Cu NWs in the polyacrylate substrates, as stated in our previous work.[33] The stability of the graphene–Cu NW hybrid film was also improved, which reflected on the lower R/R_0 ratio (1.36) after the film being kept in air for 6 months. This is because the partly-embedding of Cu NWs reduced the surface roughness of the film and improved the contact between graphene and the Cu NW film. Unfortunately, at 60 °C, the stability of graphene–Cu NW films on polyacrylate substrates was less than satisfactory.

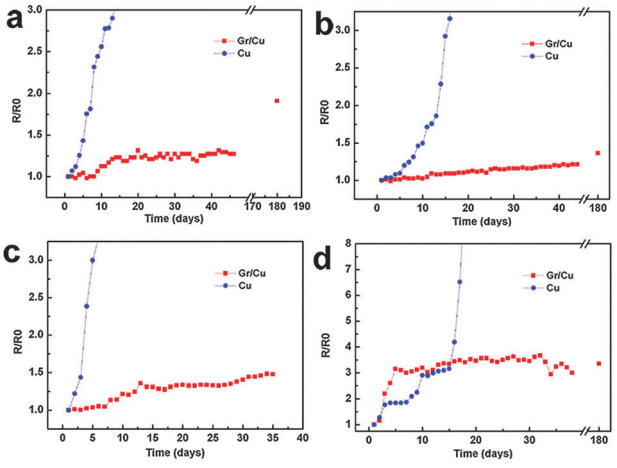

Fig. 2 Change of the resistance ratio (R/R_0) of hybrid graphene–Cu NW films on various substrates and at different temperatures. (a) Silicon substrates at room temperature. (b) Polyacrylate substrates at room temperature. (c) Silicon substrates at 60 °C. (d) Polyacrylate substrates at 60 °C.

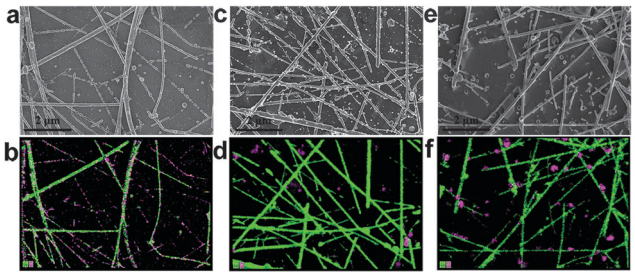

Fig. 3 SEM and *in situ* elemental surface scanning analysis of bare Cu NW films on silicon substrates exposed in an ambient atmosphere at room temperature for 35 days (a) and (b). SEM and *in situ* elemental surface scanning analysis of hybrid graphene–Cu NW films on silicon substrates stored in an ambient atmosphere for 35 days (c) and (d) at room temperature and (e) and (f) 60 °C. Green and purple colors represent Cu and O elements, respectively.

The R/R_0 ratio exceeded 2 within 3 days, and then maintained almost stable until 6 months. The deformation of the polyacrylate substrate at elevated temperature is mainly responsible for the initial increase in the sheet resistance.

Element surface scanning analysis was made to disclose the oxidation state of Cu NWs more intensively. Fig. 3a and b show the SEM image and the *in situ* elemental mapping image of a piece of bare Cu NW film exposed in an ambient atmosphere for 35 days at room temperature. A large amount of oxygen element (purple) was observed along the nanowires, and some nanowires even broke into short rods, demonstrating the heavy oxidation of the bare Cu NWs in an ambient atmosphere. In contrast, few oxygen elements were observed in the graphene–Cu NW film, and the nanowires maintained initial morphology. Even stored in an ambient atmosphere at 60 °C for 35 days, only a small amount of oxygen was observed, which was mainly assembled on big particles and around the wire–wire junctions (Fig. 3e and f). This again proved the splendid oxidation resistant effect of graphene.

2.3 Oxidation kinetics: XPS and Raman characterization

We monitored the oxidation kinetics of Cu NWs with and without graphene coverage using Raman spectra. According to previous reports, different copper oxides have distinctive Raman peaks: CuO (290, 345 cm^{-1}), Cu_2O (220 cm^{-1}), $CuCO_3{\cdot}Cu(OH)_2$ (152, 179 cm^{-1}).[34–36] As seen from Fig. 4a, no obvious oxide peaks appeared in the fresh Cu NW film while a weak Cu_2O peak was observed in the graphene covered Cu NW film. This is reasonable since the wet process of making graphene covered Cu NW film will induce slight oxidation of the Cu NWs. After four days aging in an ambient atmosphere, CuO and Cu_2O were detected in both bare Cu NW film and graphene covered Cu NW film. Somewhat differently, CuO was the primary oxide in the bare Cu NW film, while in graphene covered Cu NW film, Cu_2O was dominated. With the prolonging of aging time, the intensity ratio of CuO to Cu_2O in the spectrum of the bare Cu NW film became larger, indicating further oxidation of Cu NWs, and almost all of the Cu_2O turned into CuO after aging for 35 days. In contrast, the dominant oxides in the

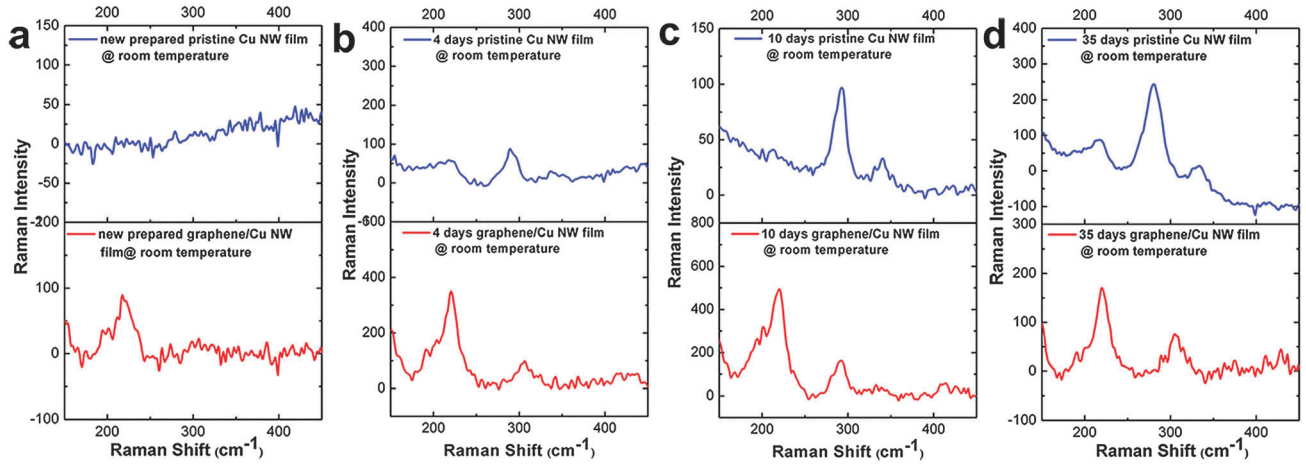

Fig. 4 Raman spectra of pristine Cu NW films (above) and hybrid graphene–Cu NW films (bottom) on silicon substrates kept at room temperature for 0 days (a), 4 days (b), 10 days (c) and 35 days (d).

graphene covered Cu NW film maintained Cu_2O, without further oxidation.

The Cu $2p_{3/2}$ XPS spectral analysis of the aged Cu NW film with and without graphene coverage affirmed the results of Raman characterization. The XPS peaks of Cu(0) and Cu(I) (Cu_2O) differ by only 0.1 eV and cannot be resolved by most XPS instruments. However, Cu(II) species have a significant peak shift and two strong shakeup satellites. Fig. 5a shows the spectrum of the fresh Cu NW film. The high-intensity peak at ~932.7 eV was assigned to the overlap of Cu and Cu_2O, and the low-intensity peak at ~934.8 eV was assigned to $Cu(OH)_2$, while no satellite peak of CuO was found at about 940–945 eV. After aging in an ambient atmosphere for 35 days, the Cu $2p_{3/2}$ peak upshifted to 935.6 eV and strong CuO satellite peaks were observed, indicating the high level oxidation of Cu NWs. In contrast, for the graphene covered Cu NW film, the Cu $2p_{3/2}$ peak remained at 932.7 eV and only slight CuO shakeup satellites appeared at 940.2 and 943.5 eV. Raman and XPS analysis disclosed that bare Cu NWs would be oxidized to Cu_2O firstly when aged in an ambient atmosphere, and then turned into CuO with the prolonging of aging time. The oxidation process proceeds continuously, causing the nanowires lose their conductance. The graphene layer can prevent further oxidation of Cu_2O, and keep most of the nanowires in the state of Cu(0) with a thin layer of Cu(I).

2.4 Mechanism of the oxidation resistance function of graphene on Cu NW films

Based on the above analysis, graphene can work as an oxygen barrier and protect the underlying Cu NW film from oxidation for a long time. This is different from previous reports, in which graphene was considered to offer effective short-term oxidation protection, but to promote wet corrosion of Cu foils over long time scales. Unlike the flat surface of the Cu foil, the Cu NW film is a rough network with peaks (junctions and particles) and valleys (downward nanowires and open space). Those protruding particles will isolate the graphene layer from Cu NWs, hindering their intact contact. Therefore, the electron transfer from Cu NWs to the graphene layer was not as effective as in the copper foil–graphene samples. Besides, during the process of introducing graphene, Cu NWs were slightly oxidized, as disclosed by Raman spectra. The thin Cu_2O layer also hindered the electron transport from Cu NWs to graphene. These two reasons mainly answered why graphene did not accelerate the oxidation of Cu NWs in this work.

As shown in Scheme 2, compared with the copper foil, Cu NWs are with higher surface energy and are more easily oxidized, which resulted in a significant increase in the sheet resistance in an ambient atmosphere. Their oxidation process mainly consisted of two steps as shown in Scheme 2: first,

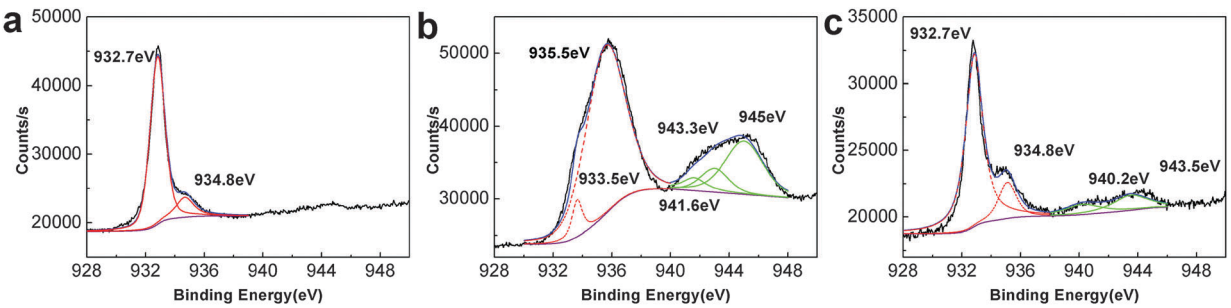

Fig. 5 Cu $2p_{3/2}$ XPS spectrum of new-prepared pristine Cu NW film (a) and of bare Cu NW film on silicon substrates kept at room temperature for 35 days (b) and of hybrid graphene–Cu NW films on silicon substrates kept at room temperature for 35 days (c).

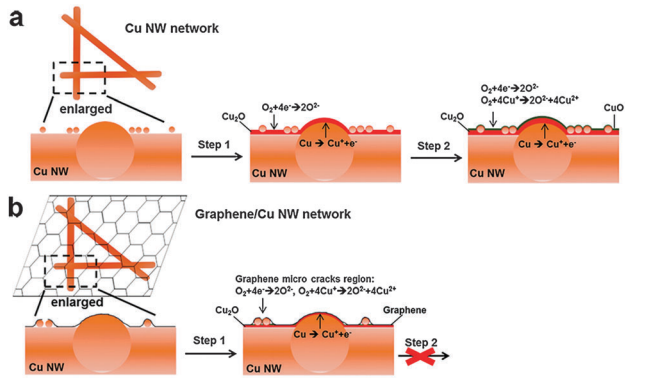

Scheme 2 Oxidation mechanism of Cu NW films (a) in the absence and (b) presence of graphene films.

from Cu to Cu_2O; second, from Cu_2O to CuO and $CuCO_3{\cdot}Cu(OH)_2$. As the Cu_2O layer becomes thicker, the first step will be limited by the slow migration of Cu^+ and electrons, thereafter the second step dominates. After covering with graphene, Cu NWs were isolated from an ambient atmosphere, however, the oxidation from Cu to Cu_2O (step 1) also occurred as confirmed by Raman and XPS analysis, which should be attributed to the bleed of O_2 and H_2O through the defects on the graphene. As discussed above, Cu NW films are rough networks with protruding particles, which will bring in a significant topography change to the above graphene layer and induce defects or even micro-cracks. O_2 and H_2O bleed through the defects would cause the prior oxidation of these areas, which had been observed from the SEM elemental mapping images (Fig. 3a and b). The partial oxidation of Cu NWs caused the slight increase in the sheet resistance. Fortunately, further oxidation of Cu_2O to CuO (step 2) barely occurred due to the limited O_2 and H_2O under the graphene layer. Upon prolonging aging time, the Cu_2O layer turned thicker, resulting in slower and slower oxidation kinetics. Therefore, the sheet resistance of the graphene covered Cu NW film increased very slowly. Elevating temperature will accelerate the migration of ions and charges, resulting in faster oxidation of Cu NWs and a faster increase in the sheet resistance.

Based on the above analysis, the main function of graphene is preventing the permeation of O_2 and H_2O, decelerating the oxidation from Cu to Cu_2O and hindering the oxidation Cu_2O to CuO. Reducing the defects on graphene or introducing multi-layers of graphene is expected to play a better role in protecting the underlying Cu NWs and is underway in our group.

3. Conclusions

In this work, we fabricated graphene covered Cu NW films and demonstrated the long term oxidation resistant effect of graphene on the underlying Cu NW network. Besides, we proposed the two-step oxidation kinetics of Cu NWs and discovered the anti-oxidation mechanism of graphene on Cu NWs particularly. Moreover, graphene with fewer defects or with multilayers was expected to be more effective as an oxidation barrier and will be investigated in our future work. The results obtained in this work are of referring significance to make metal nanowire based transparent electrodes with both high optical-electrical performance and excellent stability.

4. Experimental

4.1 Fabrication of Cu NW films on silicon substrates

Cu NWs were fabricated according to the procedure proposed by our group.[12] The films were prepared using a vacuum filtration method. Typically, Cu NWs were dispersed in toluene by bath sonication for 1–2 min, and then filtered onto a nitrocellulose filter membrane. After filtration, the membranes were transferred onto a silicon substrate, dried under vacuum at 80 °C for 2 h, and then dipped in acetone for 30 min to dissolve the filtration membrane; leaving copper nanowire based thin films on the silicon substrate. Finally, the films were treated under hydrogen gas at 300 °C to remove the oxidized layers and the residue organics from the surface.

4.2 Fabrication of Cu NW films on polyacrylate substrates

Cu NW films were firstly fabricated on glass substrates with the same procedure, then a layer of acrylate monomers was coated onto the films by dip coating, followed by UV-irradiation for 3–5 minutes. At last, the glass substrate was separated and Cu NW films on polyacrylate substrates were obtained.

4.3 Construction of graphene–Cu NW hybrid films

Graphene was grown on a 25 μm thick copper foil using an ambient pressure chemical vapor deposition (CVD) technique with methane as a carbon source by the same procedure reported in our previous study.[37,38] A wet transfer technique was used to transfer graphene onto the Cu NW film. Typically, a layer of PMMA was spun onto the graphene covered copper foil, and then the copper foil was etched away with a copper etchant (0.1 M $(NH_4)_2S_2O_8$). The resulting floating PMMA–graphene stack was rinsed with DI water several times in order to remove the residual etchant and then transferred onto Cu NW films in a mixture of glycol–water solution, followed by a treatment at 120 °C in a hydrogen atmosphere. The supporting PMMA was finally removed away with acetone rinsing and the resulting graphene–Cu NW film was dried at room temperature (25 °C) overnight.

4.4 Characterization of graphene–Cu NW films

For the room temperature test, the samples were put in the constant temperature (25 °C) room and the environment humidity is 39%. For the high temperature test, the samples were put in the 60 °C oven, and the humidity is 16%. The sheet resistances of all samples were measured using a four point resistance meter with silver paste as the contact pad. FE-SEM and elemental mapping scanning analysis were observed using a Magellan 400 microscope using 2.0 or 5.0 kV acceleration voltage. Optical transmittances of graphene–Cu NW films were measured using a Perkin Elmer Lambda 950 UV-vis spectrometer. XPS spectra were observed using a Thermo Scientific ESCALAB 250Xi X-ray Photoelectron Spectrometer to measure

the atom species. Deconvolution of XPS spectra was obtained resolved by fitting each peak with a combined Guassian–Lorentzian function after background subtraction. Raman measurements were carried out to study graphene and the oxidation of Cu NW films by using a 532 nm laser under ambient conditions with a Raman microscope (Thermo Scientific Raman DXR), and the laser spot and power size were ~0.7 μm and 8 mW.

Acknowledgements

This work was supported by the National Basic Research Program of China (2012CB932303) and the National Natural Science Foundation of China (Grant No. 61301036, 51072215), STC of Shanghai (Grant No. 13ZR1463600), and Innovation Foundation of SICCAS.

Notes and references

1 R. Bel Hadj Tahar, T. Ban, Y. Ohya and Y. Takahashi, *J. Appl. Phys.*, 1998, **83**, 2631–2645.
2 J. Burroughes, D. Bradley, A. Brown, R. Marks, K. Mackay, R. Friend, P. Burns and A. Holmes, *Nature*, 1990, **347**, 539–541.
3 Y. Zhu, Z. Z. Sun, Z. Yan, Z. Jin and J. M. Tour, *ACS Nano*, 2011, **5**, 6472–6479.
4 P. B. Catrysse and S. H. Fan, *Nano Lett.*, 2010, **10**, 2944–2949.
5 G. Yu, A. Cao and C. M. Lieber, *Nat. Nanotechnol.*, 2007, **2**, 372–377.
6 J.-U. Park, M. A. Meitl, S.-H. Hur, M. L. Usrey, M. S. Strano, P. J. A. Kenis and J. A. Rogers, *Angew. Chem., Int. Ed.*, 2006, **45**, 581–585.
7 Z. Wu, Z. Chen, X. Du, J. M. Logan, J. Sippel, M. Nikolou, K. Kamaras, J. R. Reynolds, D. B. Tanner, A. F. Hebard and A. G. Rinzler, *Science*, 2004, **305**, 1273–1276.
8 J.-U. Park, S. Nam, M.-S. Lee and C. M. Lieber, *Nat. Mater.*, 2012, **11**, 120–125.
9 J.-H. Chen, C. Jang, S. Xiao, M. Ishigami and M. S. Fuhrer, *Nat. Nanotechnol.*, 2008, **3**, 206–209.
10 X. S. Li, Y. w. Zhu, W. W. Cai, M. Borysiak, B. Y. Han, D. Chen, R. D. Piner, L. Colombo and R. S. Ruoff, *Nano Lett.*, 2009, **9**, 4359–4363.
11 C. M. Lieber, *MRS Bull.*, 2011, **36**, 1052–1063.
12 D. Q. Zhang, R. R. Wang, M. C. Wen, D. Weng, X. Cui, J. Sun, H. X. Li and Y. F. Lu, *J. Am. Chem. Soc.*, 2012, **134**, 14283–14286.
13 C. Wang, Y. J. Hu, C. M. Lieber and S. H. Sun, *J. Am. Chem. Soc.*, 2008, **130**, 8902–8903.
14 S. De, T. M. Higgins, P. E. Lyons, E. M. Doherty, P. N. Nirmalraj, W. J. Blau, J. J. Boland and J. N. Coleman, *ACS Nano*, 2009, **3**, 1767–1774.
15 L. Q. Yang, T. Zhang, H. X. Zhou, S. C. Price, B. J. Wiley and W. You, *ACS Appl. Mater. Interfaces*, 2011, **3**, 4075–4084.
16 H. Wu, L. B. Hu, M. W. Rowell, D. S. Kong, J. J. Cha, J. R. McDonough, J. Zhu, Y. Yang, M. D. McGehee and Y. Cui, *Nano Lett.*, 2010, **10**, 4242–4248.
17 P. E. Lyons, S. De, J. Elias, M. Schamel, L. Philippe, A. T. Bellew, J. J. Boland and J. N. Coleman, *J. Phys. Chem. Lett.*, 2011, **2**, 3058–3062.
18 D.-S. Leem, A. Edwards, M. Faist, J. Nelson, D. D. C. Bradley and J. C. de Mello, *Adv. Mater.*, 2011, **23**, 4371–4375.
19 L. B. Hu, H. S. Kim, J. Y. Lee, P. Peumans and Y. Cui, *ACS Nano*, 2010, **4**, 2955–2963.
20 W. L. Hu, X. F. Niu, L. Li, S. Yun, Z. B. Yu and Q. B. Pei, *Nanotechnology*, 2012, **23**, 344002.
21 M. S. Miller, J. C. O'Kane, A. Niec, R. S. Carmichael and T. B. Carmichael, *ACS Appl. Mater. Interfaces*, 2013, **5**, 10165–10172.
22 Y. Wu, J. Xiang, C. Yang, W. Lu and C. M. Lieber, *Nature*, 2004, **430**, 61–65.
23 A. R. Rathmell, M. Nguyen, M. F. Chi and B. J. Wiley, *Nano Lett.*, 2012, **12**, 3193–3199.
24 R. Zhu, C.-H. Chung, K. C. Cha, W. Yang, Y. B. Zheng, H. Zhou, T.-B. Song, C.-C. Chen, P. S. Weiss, G. Li and Y. Yang, *ACS Nano*, 2011, **5**, 9877–9882.
25 W. Gaynor, G. F. Burkhard, M. D. McGehee and P. Peumans, *Adv. Mater.*, 2011, **23**, 2905–2910.
26 M. Cox, A. Gorodetsky, B. J. Kim, K. S. Kim, Z. Jia, P. Kim, C. Nuckolls and I. Kymissis, *Appl. Phys. Lett.*, 2011, **98**, 123303.
27 Y. Y. Zhang, L. C. Wang, X. Li, X. Y. Yi, N. Zhang, J. Li, H. W. Zhu and G. H. Wang, *J. Appl. Phys.*, 2012, **111**, 114501.
28 J. O. Hwang, J. S. Park, D. S. Choi, J. Y. Kim, S. H. Lee, K. E. Lee, Y.-H. Kim, M. H. Song, S. Yoo and S. O. Kim, *ACS Nano*, 2011, **6**, 159–167.
29 S. Koichi, W. Shunichiro, G. Takuya and U. Keiji, *Appl. Phys. Express*, 2011, **4**, 021603.
30 D. Prasai, J. C. Tuberquia, R. R. Harl, G. K. Jennings and K. I. Bolotin, *ACS Nano*, 2012, **6**, 1102–1108.
31 F. Zhou, Z. Li, G. J. Shenoy, L. Li and H. Liu, *ACS Nano*, 2013, **7**, 6939–6947.
32 W. R. Maria Schriver, W. J. Gannett, A. M. Zaniewski, M. F. Crommie and A. Zettl, *ACS Nano*, 2013, **7**, 5763–5768.
33 Y. Cheng, S. L. Wang, R. R. Wang, J. Sun and L. Gao, *J. Mater. Chem. C*, 2014, **2**, 5309.
34 S. L. Shinde and K. K. Nanda, *RSC Adv.*, 2012, **2**, 3647–3650.
35 F. Texier, L. Servant, J. L. Bruneel and F. Argoul, *J. Electroanal. Chem.*, 1998, **446**, 189–203.
36 B. L. Hurley and R. L. McCreery, *J. Electrochem. Soc.*, 2003, **150**, B367–B373.
37 F. Yang, Y. Liu, W. Wu, W. Chen, L. Gao and J. Sun, *Nanotechnology*, 2012, **23**, 475705.
38 L. J. Shi, Y. Q. Liu, F. Yang, L. Gao and J. Sun, *Nanotechnology*, 2014, **25**, 145704.

